Article

Triplet-State Formation along the Ultrafast Decay of Excited Singlet Cytosine

Manuela Merchn, Luis Serrano-Andrs, Michael A. Robb, and Llus Blancafort

J. Am. Chem. Soc., **2005**, 127 (6), 1820-1825• DOI: 10.1021/ja044371h • Publication Date (Web): 21 January 2005

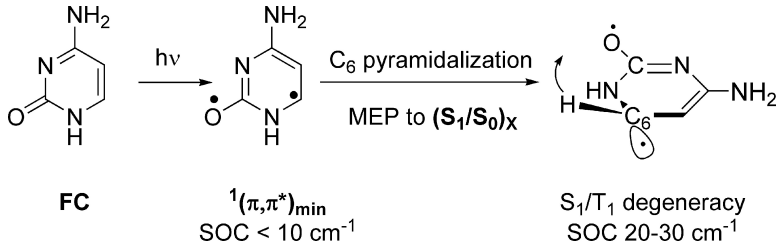

More About This Article

Additional resources and features associated with this article are available within the HTML version:

- Supporting Information
- Links to the 12 articles that cite this article, as of the time of this article download
- Access to high resolution figures
- Links to articles and content related to this article
- Copyright permission to reproduce figures and/or text from this article

View the Full Text HTML

J|A|C|S
ARTICLES
Published on Web 01/21/2005

Triplet-State Formation along the Ultrafast Decay of Excited Singlet Cytosine

Manuela Merchán,[†] Luis Serrano-Andrés,*[,†] Michael A. Robb,[‡] and Lluís Blancafort*[,§]

Contribution from the Instituto de Ciencia Molecular, Universitat de València, Dr. Moliner 50, Burjassot, ES-46100 Valencia, Spain, Department of Chemistry, Imperial College London, London SW7 2AZ, United Kingdom, and Institut de Química Computacional, Departament de Química, Universitat de Girona, ES-17071 Girona, Spain

Received September 16, 2004; E-mail: lluis.blancafort@udg.es(L.B.); Luis.Serrano@uv.es(L.S.A.)

Abstract: We address the possibility of populating the lowest triplet state of cytosine by an "intrinsic" mechanism, namely, intersystem crossing (ISC) along the ultrafast internal conversion pathway of the electronically excited singlet species. For this purpose, we present a discussion of the ISC process and triplet-state reactivity based on theoretical analysis of the spin−orbit strength and the potential energy surfaces for the relevant singlet and triplet states of cytosine. High-level ab initio computations show that ISC is possible in wide regions of the singlet manifold along the reaction coordinate that controls the ultrafast internal conversion to the ground state. Thus, the ISC mechanism documented here provides a possibility to access the triplet state, which has a key role in the photochemistry of the nucleic acid bases.

Introduction

Significant advances in understanding the singlet-state photophysics of the nucleic acid bases have occurred in recent years. Light absorption initially produces excited states of singlet multiplicity having a high photostability as their most remarkable characteristics, due to ultrafast decay pathways for electronic energy. Fluorescence lifetimes of DNA/RNA nucleosides and nucleotides measured in solution by several groups fall in the subpicosecond time scale, suggesting the presence of an ultrafast internal conversion channel (for a recent review, see ref 1). Very short lifetimes, in the picosecond regime, have also been determined in the gas phase for the isolated purine and pyrimidine bases.[2] Such favorable internal conversion (IC) processes behave in these molecules as a self-protection mechanism preventing photochemical reactions induced by UV radiation. Computational results[3−5] for cytosine have shown that the ultrafast decay is due to the presence of an energetically accessible region of conical intersection between the lowest excited and the ground state.

Along the ultrafast internal conversion of singlet-excited cytosine, the lowest triplet state might be populated by an intersystem crossing (ISC) mechanism. Such a possibility is explored in the present contribution and has been the main underlying reason to undertake the current research. Despite the fact that triplet formation has a low quantum yield (≤ 0.01 in water),[6] longer-lived triplet states are crucial when considering the DNA chemistry. Their relevant role in the photochemistry and photophysics of the DNA components is well-known because they are precursors of the cyclobutadipyrimidines.[6] These compounds are formed through the dimerization of pyrimidinic thymine and cytosine derivatives after UV irradiation mediated by ISC from the singlet to the triplet state. Dimerization is observed in DNA models, such as the isolated bases in solution and oligonucleotides, and also in naked and cellular DNA, where it is believed to be one of the major photochemical events.[6−8] Moreover, recent theoretical results from one of our group suggest that the triplet state may also induce phototautomerization in Watson−Crick pairs.[9]

Despite great experimental efforts, the initial formation of the photoreactive triplet state has not been explained satisfactorily. One of the mechanisms proposed in the literature involves triplet energy transfer from "external" photosensitizers added to the DNA or from "endogenous" sensitizers present in the cell.[8] Here, we show that along the ultrafast fluorescence decay, nonsensitized population of the triplet state through ISC between

[†] Universitat de València.
[‡] Imperial College London.
[§] Universitat de Girona.

(1) Crespo-Hernández, C. E.; Cohen, B.; Hare, P. M.; Kohler, B. *Chem. Rev.* **2004**, *104*, 1977−2019.
(2) Kang, H.; Lee, K. T.; Jung, B.; Ko, Y. J.; Kim, S. K. *J. Am. Chem. Soc.* **2002**, *124*, 12958−12959.
(3) Blancafort, L.; Robb, M. A. *J. Phys. Chem. A* **2004**, *108*, 10609−10614.
(4) Merchán, M.; Serrano-Andrés, L. *J. Am. Chem. Soc.* **2003**, *125*, 8108−8109.
(5) Ismail, N.; Blancafort, L.; Olivucci, M.; Kohler, B.; Robb, M. A. *J. Am. Chem. Soc.* **2002**, *124*, 6818−6819.
(6) Cadet, J.; Vigny, P. In *Bioorganic Photochemistry*; Morrison, H., Ed.; John Wiley & Sons: New York, 1990; Vol. 1, pp 1−272.
(7) Douki, T.; Cadet, J. *Biochemistry* **2001**, *40*, 2495−2501.
(8) Douki, T.; Reynaud-Angelin, A.; Cadet, J.; Sage, E. *Biochemistry* **2003**, *42*, 9221−9226.
(9) Blancafort, L.; Sodupe, M.; Bertran, J. *J. Am. Chem. Soc.* **2004**, *126*, 12770−12771.

10.1021/ja044371h CCC: $30.25

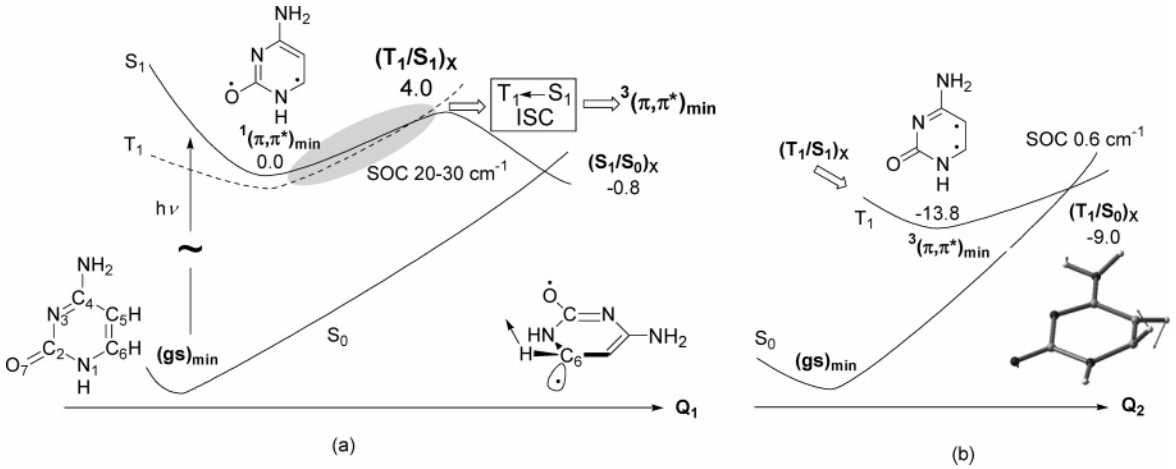

Figure 1. Cuts along the potential-energy surfaces of S_0, S_1, and T_1, showing the proposed route for the triplet-state formation along the minimum-energy path for ultrafast decay of electronically excited singlet cytosine (a) and the nonradiative deactivation mechanism of $^3(\pi,\pi^*)_{min}$ (b). (Energies are in kcal mol^{-1}, SOC is in cm^{-1}.)

the lowest singlet excited (S_1) and the lowest triplet state (T_1) is possible for cytosine, providing a mechanism of "intrinsic" triplet sensitization of the base. It is worth mentioning in this context that the ISC yields at room temperature for the pyrimidine bases, estimated by various techniques, fall within the range of $10^{-2}-10^{-3}$, approximately, and triplet emission is also observed in low-temperature matrix experiments.[10] Moreover, rather long-lived, dark excited states, with lifetimes of hundreds of nanoseconds, have been detected by resonantly enhanced multiphoton ionization (REMPI) experiments for cytosine[11] and thymine[12,13] in the gas phase. Both a triplet state and an (n,π^*) singlet state have been proposed earlier as possible candidates of the observed dark states, and our present computations give support in favor of the triplet state as the actual dark species detected experimentally.

Our CASPT2//CASSCF results are summarized in Figure 1, where we present the two main points of interest. Figure 1a shows the population of the triplet state after initial singlet excitation. The first part of the decay on the singlet-state surface leads to the excited-state minimum, $^1(\pi,\pi^*)_{min}$. From there on, the singlet and triplet excited states (S_1 and T_1, respectively) are almost degenerate along the minimum-energy path (MEP) to the region responsible for the ultrafast decay of the singlet state (path from $^1(\pi,\pi^*)_{min}$ to $(S_1/S_0)_X$). Along this path, there is substantial spin−orbit coupling (SOC) (20−30 cm^{-1}). Together with the small singlet−triplet energy gap, this allows for the occurrence of ISC from S_1 to T_1. Clearly, the decay to S_0 is more efficient because it does not involve a change of spin and it dominates over the ISC. However, the experimental results described above show that the triplet state, despite its low quantum yields, is relevant for the photochemistry of the DNA pyrimidine bases, and our present results explain the triplet-state formation. Similar to its important role in the singlet-state photophysics,[3−5] the C_6 pyramidalization is essential in favoring the ISC because it induces an increase of the SOC along the coordinate. The second point is the fate of the triplet (Figure 1b). After the ISC, the molecule decays to the equilibrium structure for the lowest triplet state, $^3(\pi,\pi^*)_{min}$, where the excitation is localized on the C_5-C_6 π bond of cytosine. This biradical species can react further or decay to the ground state, either by radiative emission (phosphorescence) or by nonradiative decay via ISC with S_0.

Computational Details

Vertical Excitations and Potential Energy Surfaces. The well-established CASPT2//CASSCF protocol was used throughout our calculations.[14] The calculation of the critical points and MEP with Molcas-6[15] and Gaussian03[16] is reported in the Supporting Information. The CASPT2 calculations were carried out with Molcas-6,[15] using a CASSCF(12,9)/6-31G(d,p) zero-order wave function unless otherwise stated. The active space includes seven π orbitals (all except the MO localized on the NH_2 group) and the two lone pairs (located on the N_3 and oxygen atoms, n_N and n_O hereafter). The core orbitals were not correlated, and the so-called imaginary level-shift technique[3] was employed with IMAG = 0.2 au. The states of interest were obtained from average CASSCF(12,9) calculations, using five roots for the states of singlet multiplicity and six roots for the triplet states. Therefore, an equivalent computational treatment was given to the vertical excitation energies and to the calculated band origins. To reduce computational effort, the CASPT2 energies along the minimum-energy path (MEP) for singlet state decay (Figure 3) were calculated only for the three lowest singlets and the two lowest triplets, due to the large separation between these states and the higher lying ones along the path. These

(10) Görner, H. *J. Photochem. Photobiol. B* **1990**, *5*, 359−377.
(11) Nir, E.; Muller, M.; Grace, L. I.; de Vries, M. S. *Chem. Phys. Lett.* **2002**, *355*, 59−64.
(12) He, Y. G.; Wu, C. Y.; Kong, W. *J. Phys. Chem. A* **2003**, *107*, 5145−5148.
(13) He, Y. G.; Wu, C. Y.; Kong, W. *J. Phys. Chem. A* **2004**, *108*, 943−949.
(14) Merchán, M.; Serrano-Andrés, L.; Fülscher, M. P.; Roos, B. O. In *Recent Advances in Multireference Methods*;Hirao, K., Ed.; World Scientific Publishing: Singapore, 1999.
(15) Andersson, K.; Barysz, M.; Bernhardsson, A.; Blomberg, M. R. A.; Carissan, Y.; Cooper, D. L.; Cossi, M.; Fülscher, M. P.; Gagliardi, L.; de Graaf, C.; Hess, B.; Hagberg, G.; Karlström, G.; Lindh, R.; Malmqvist, P.-Å.; Nakajima, T.; Neogrády, P.; Olsen, J.; Raab, J.; Roos, B. O.; Ryde, U.; Schimmelpfennig, B.; Schütz, M.; Seijo, L.; Serrano-Andrés, L.; Siegbahn, P. E. M.; Stålring, J.; Thorsteinsson, T.; Veryazov, V.; Widmark, P.-O. *MOLCAS*, version 6.0; Department of Theoretical Chemistry, Chemical Centre, University of Lund: Lund, Sweden, 2004.
(16) Frisch, M. J.; Trucks, G. W.; Schlegel, H. B.; Scuseria, G. E.; Robb, M. A.; Cheeseman, J. R.; Zakrzewski, V. G.; Montgomery, J. A., Jr.; Stratmann, R. E.; Burant, J. C.; Dapprich, S.; Millam, J. M.; Daniels, A. D.; Kudin, K. N.; Strain, M. C.; Farkas, O.; Tomasi, J.; Barone, V.; Cossi, M.; Cammi, R.; Mennucci, B.; Pomelli, C.; Adamo, C.; Clifford, S.; Ochterski, J.; Petersson, G. A.; Ayala, P. Y.; Cui, Q.; Morokuma, K.; Malick, D. K.; Rabuck, A. D.; Raghavachari, K.; Foresman, J. B.; Cioslowski, J.; Ortiz, J. V.; Stefanov, B. B.; Liu, G.; Liashenko, A.; Piskorz, P.; Komaromi, I.; Gomperts, R.; Martin, R. L.; Fox, D. J.; Keith, T.; Al-Laham, M. A.; Peng, C. Y.; Nanayakkara, A.; González, C.; Challacombe, M.; Gill, P. M. W.; Johnson, B.; Chen, W.; Wong, M. W.; Andrés, J. L.; Head-Gordon, M.; Replogle, E. S.; Pople, J. A.; *Gaussian 98*, revision A.6; Gaussian, Inc.: Pittsburgh, PA, 1998.

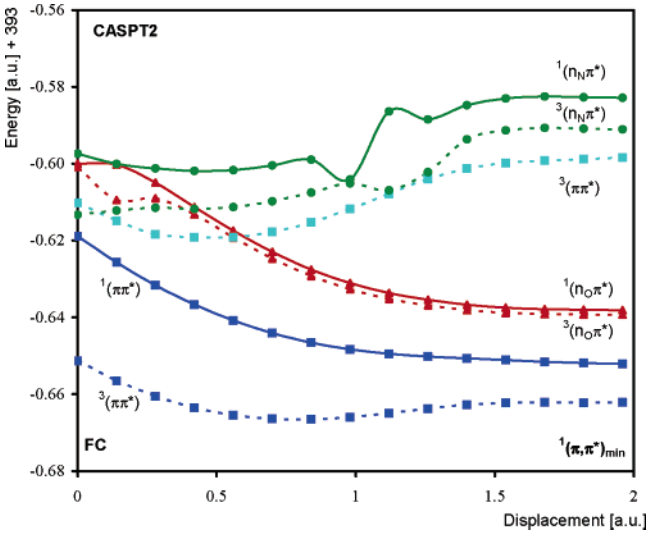

Figure 2. Evolution of the low-lying singlet and triplet excited states along the $S_1(\pi,\pi^*)$ MEP computed at the CASPT2//CASSCF level.

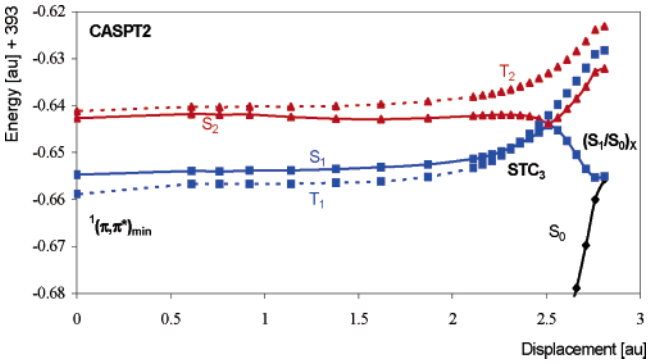

Figure 3. Energies (CASPT2//CASSCF) of the low-lying singlet and triplet excited states along the MEP from $^1(\pi,\pi^*)_{min}$ to $(S_1/S_0)_X$.

calculations were done with a smaller 6-31G(d) basis, and comparison with the energies obtained along a linear interpolation coordinate with the 6-31G(d,p) basis (five singlet and six triplet states) gives a qualitatively similar profile (see Supporting Information). In fact, one of the previous publications on the excited state of cytosine has shown that the influence of p-polarization functions on the hydrogen atoms is small.[4]

Spin−Orbit Coupling (SOC) Calculations. The SOC strength between selected states was computed as

$$SOC_{lk} = \sqrt{\sum_u |\langle T_{l,u}|\hat{H}_{SO}|S_k\rangle|^2} \quad u = x, y, z$$

which can be considered the length of the spin−orbit coupling vector $\mathbf{SOC}_{lk}$ with component $\langle T_{l,u}|\hat{H}_{SO}|S_k\rangle$. The algorithms implemented in the Molcas-6[15] and Gaussian-03[16] quantum-chemistry programs were employed. A CASSCF(12,9)/6 31G(d,p) wave function averaged over five singlet and six triplet states was used. To reduce the computational effort, the SOC along the MEP for singlet-state decay (Figure 4) was calculated with a CASSCF(12,9)/6 31G(d) wave function over three singlet and two triplet states (see above). A detailed analysis of the SOC is given in the Supporting Information.

Calculation of Radiative Lifetimes. From the calculated CASSCF transition dipole moments (TDM) and the CASPT2 excitation energies, the radiative lifetimes have been estimated by using the Strickler−Berg relationship.[17] In particular, the S−T TDMs were obtained by the following expression:

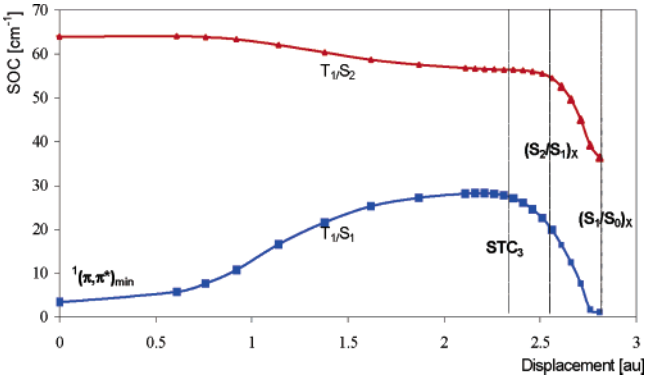

Figure 4. SOC between T_1 and S_1 and T_1 and S_2 pairs of states at CASSCF level, along MEP to S_1/S_0 crossing.

$$TDM_{ST} = \langle S|r^l|T^k\rangle = \sum_n \frac{\langle S^0|r^l|S_n^0\rangle\langle S_n^0|H_{SO}^k|T^{k,0}\rangle}{E(T^0) - E(S_n^0)} + \sum_m \frac{\langle S^0|H_{SO}^k|T_m^{k,0}\rangle\langle T_m^{k,0}|r^l|T^{k,0}\rangle}{E(S^0) - E(T_m^0)}$$

Estimation of Probability for ISC (P^{ISC}). In the semiclassical picture based on potential-energy surfaces, the probability of ISC for a molecule passing through a singlet−triplet crossing, in a Landau−Zener type model,[18] is given by

$$P^{ISC} = 1 - P^{LZ}$$

$$P^{LZ} = \exp\left(-\frac{\pi}{4}\xi\right)$$

$$\xi = \frac{8H_{SOC}^2}{\hbar\mathbf{g}\vec{\mathbf{d}}\vec{\mathbf{v}}N_{Av}}$$

Here, $\vec{\mathbf{gd}}$ is the gradient difference vector between the singlet and triplet states and $\vec{\mathbf{v}}$ the velocity of the molecule at the crossing point (see Supporting Information for details).

Results and Discussion

Triplet-State Formation (ISC from S_1 to T_1). The photophysics of electronically excited singlet cytosine at long wavelength consists of a (π,π^*) absorption feature with a minimum on the S_1 surface, $^1(\pi,\pi^*)_{min}$, and decay at a region of degeneracy with the ground state (conical intersection $(S_1/S_0)_X$; see Figure 1). On the potential-energy surface, the population transfer to the triplet state will most likely occur after decay to the minimum of the spectroscopic excited state. Ideally, large SOC occurs when the electronic transition that accompanies the spin flip creates orbital angular momentum. In the present case, where the excitation involves mainly p orbitals, the two p orbitals must be orthogonal to each other.[19] For cytosine, this implies that the population of the triplet cytosine surface could be associated to a transition between the $^1(\pi,\pi^*)$ and $^3(n_O,\pi^*)$ states since in the regions of interest (MEP

(17) Strickler, S. J.; Berg, R. A. *J. Chem. Phys.* **1962**, *37*, 814.
(18) Manaa, M. R.; Yarkony, D. R. *J. Chem. Phys.* **1991**, *95*, 1808−1816.
(19) Salem, L. *Electrons in Chemical Reactions: First Principles*; John Wiley & Sons: New York, 1982.

Table 1. Computed Spectroscopic Properties for the Low-Lying Singlet and Triplet Excited States of Cytosine at the CASPT2//CASSCF(12,9)/6-31G(d,p) Level[a]

	Vertical Transition (eV)		Band Origin (T_e, eV)		
state	CASSCF	CASPT2[b]	CASSCF	CASPT2	τ_{rad}
$^1(\pi,\pi^*)$	5.32	4.53 (0.065)	3.93	3.64	33 ns
$^1(n_O,\pi^*)$	5.34	5.04 (0.001)	3.74	3.87	1066 ns
$^1(n_N,\pi^*)$	5.67	5.11 (0.003)			
$^3(\pi,\pi^*)$	3.72	3.65	2.99	3.04	199 ms
$^3(n_N,\pi^*)$	5.19	4.68	4.01	3.89	
$^3(\pi,\pi^*)$	5.01	4.77			
$^3(n_O,\pi^*)$	5.38	5.02	3.73	3.88	

[a] Singlet-state results taken from ref 4. [b] Oscillator strength in parentheses.

for singlet-state decay), the triplet states have an electronic character similar to that in the singlet states (see the resonance structures in Figure 1a). This is in agreement with the El-Sayed selection rules for intersystem crossing.[20] On the basis of these considerations, our study considers three regions of the potential-energy surface where the ISC mechanism is possible: (1) the Franck−Condon (FC) structure $\mathbf{(gs)_{min}}$ and the MEP from $\mathbf{(gs)_{min}}$ to $\mathbf{^1(\pi,\pi^*)_{min}}$; (2) the vicinity of $\mathbf{^1(\pi,\pi^*)_{min}}$; and (3) the MEP from $\mathbf{^1(\pi,\pi^*)_{min}}$ to $\mathbf{(S_1/S_0)_X}$.

The computed spectroscopic properties for the low-lying triplet states of cytosine are listed in Table 1, where for the sake of comparison, the previously reported singlet→singlet features[4] are also included. It is clear that the lowest triplet state (T_1) is predicted to have (π,π^*) character. At the highest level of theory employed, the vertical transition for the lowest singlet→triplet electronic transition is computed to be at 3.65 eV, with the band origin at 3.04 eV. The results are consistent with the estimation of the triplet energy (3.33 eV) made for cytidine 5′-monophosphate (CMP) in aqueous solution at room temperature[21] and the recorded band maximum (around 3 eV) of the phosphorescence excitation spectrum for related compounds in polar solvents.[10] The radiative lifetime is predicted to be ∼0.2 s and is in reasonable agreement with the experimental data for the phosphorescence lifetime of cytosine (0.6−0.8 s).[10] The remaining triplet states are placed more than 1 eV above the $T_1(\pi,\pi^*)$ state, both at the FC region and at the respective equilibrium geometries. To compute the band origins, the minima for the triplet states were optimized (see Supporting Information). Interestingly, the band origins for the singlet and triplet (n_O,π^*) states are predicted to be degenerate and close to that of the $^3(n_N,\pi^*)$ state, whereas $\mathbf{^3(\pi,\pi^*)_{min}}$ is stabilized by 0.6 eV with respect to $\mathbf{^1(\pi,\pi^*)_{min}}$. The CASSCF geometry optimization of the $^3(n_N,\pi^*)$ state gives a minimum on the potential-energy surface, whereas the optimization of the $^1(n_N,\pi^*)$ state leads directly to a conical intersection with the ground state. It is worth recalling that this state is expected to play a minor role in the ultrafast decay of singlet-excited cytosine because of the relatively larger barrier height that the system has to overcome compared to that in the $^1(\pi,\pi^*)$ path.[4,5]

The evolution of the low-lying singlet and triplet states along the MEP to $\mathbf{^1(\pi,\pi^*)_{min}}$ (essentially a bond inversion coordinate in the ring)[3−5] is depicted in Figure 2. The $T_1(\pi,\pi^*)$ and T_2-(n_O,π^*) states are placed below and above S_1, respectively, along the relaxation path. As could be expected when invoking simple molecular orbital (MO) models, the $^{1,3}(n_O,\pi^*)$ states stay close. The remaining singlet and triplet states considered become progressively destabilized as the geometry change imposed along the reaction coordinate of S_1 increases. At the end of the S_1 MEP, which is essentially coincident with the $\mathbf{^1(\pi,\pi^*)_{min}}$ structure, the T_1 and T_2 states are placed at −0.28 and +0.34 eV, with respect to the energy of $\mathbf{^1(\pi,\pi^*)_{min}}$. The computed SOC in the $\mathbf{FC\text{-}^1(\pi,\pi^*)_{min}}$ region is much more pronounced for the $^1(\pi,\pi^*)/^3(n_O,\pi^*)$ pair than for the $^1(\pi,\pi^*)/^3(\pi,\pi^*)$ states. However, the singlet−triplet gap is too large for ISC to take place efficiently.

We continue with an exploration of the region of quasiplanar geometries in the region around $\mathbf{^1(\pi,\pi^*)_{min}}$, where the C_6 pyramidalization is approximately 20° or less. A quasiplanar minimum, $\mathbf{^3(n_O,\pi^*)_{min}}$, has been optimized on the T_2 surface, approximately 8.5 kcal mol^{-1} (0.37 eV) above $\mathbf{^1(\pi,\pi^*)_{min}}$. A crossing between the $^1(\pi,\pi^*)$ and $^3(n_O,\pi^*)$ states has been located near that minimum, using linear displacements (see Supporting Information), but the barrier to access the $^1(\pi,\pi^*)/^3(n_O,\pi^*)$ crossing (hereafter "singlet−triplet crossing 1", $\mathbf{STC_1}$) from $\mathbf{^1(\pi,\pi^*)_{min}}$ is high (15 kcal mol^{-1}, 0.65 eV). In addition, a $^1(\pi,\pi^*)/^3(\pi,\pi^*)$ degeneracy point ($\mathbf{STC_2}$) has been located in the vicinity of $\mathbf{^1(\pi,\pi^*)_{min}}$. The crossing has a low energy of 2.1 kcal mol^{-1} (0.09 eV) relative to that of $\mathbf{^1(\pi,\pi^*)_{min}}$, but the corresponding SOC is comparatively small (7.5 cm^{-1}). Thus, ISC at quasiplanar geometries seems unlikely either because of the high-energy barrier heights or because of the small SOC involved.

The key region of favorable ISC to T_1 is the path from $\mathbf{^1(\pi,\pi^*)_{min}}$ to $\mathbf{(S_1/S_0)_X}$ (shaded region in Figure 1a), which corresponds to bond inversion and pyramidalization of C_6.[3−5] The energies of the lowest-lying singlet and triplet states (CASPT2//CASSCF/6-31G(d) results; see Computational Details) are shown in Figure 3 and the corresponding SOC values in Figure 4. The S_1-T_1 energy gap (Figure 3) remains small along a large part of the path. A further point of S_1/T_1 degeneracy ($\mathbf{STC_3}$) lies along the path at 4 kcal mol^{-1} (0.17 eV) above $\mathbf{^1(\pi,\pi^*)_{min}}$. For comparison, the estimated barrier to access $\mathbf{(S_1/S_0)_X}$ from $\mathbf{^1(\pi,\pi^*)_{min}}$ is higher (approximately 7 kcal mol^{-1} or 0.3 eV; see Figure 3). These results strongly suggest that close to the MEP for singlet-state decay there is a seam of S_1/T_1 intersection anchored on the $\mathbf{STC_2}$ and $\mathbf{STC_3}$ crossing points. The increase of SOC between the S_1/T_1 states along the path from $\mathbf{^1(\pi,\pi^*)_{min}}$ to $\mathbf{(S_1/S_0)_X}$ is shown in Figure 4. Examination of the calculated values (see Supporting Information) shows that the high SOC comes from the "mixed" $(\pi,\pi^*)/(n_O,\pi^*)$ character of the states along the MEP, induced by the pyramidalization of C_6.[3] This underlines the importance of the pyramidalization in favoring the ISC from S_1 to T_1.

To get an estimate of the probability of ISC from S_1 to T_1, the rate constant, k_{ISC}, for nonradiative ISC from a triplet (T) to a singlet (S) state can be obtained, in principle, from Fermi's Golden Rule:

$$k_{ISC} = \frac{2\pi}{\hbar}|\langle T|\hat{H}_{SO}|S\rangle|^2\rho(E)$$

where $\hat{H}_{SO}$ is the spin−orbit coupling operator and $\rho(E)$ is the density of states in the final electronic states.[22] However, in

(20) Lower, S. K.; El-Sayed, M. A. *Chem. Rev.* **1966**, *66*, 199−241.
(21) Wood, P. D.; Redmond, R. W. *J. Am. Chem. Soc.* **1996**, *118*, 4256−4263.

the present work, we use a semiclassical picture based on potential-energy surfaces, where the probability for ISC, P^{ISC}, is given by the Landau−Zener-type model given in the Computational Details. This approach is appropriate to estimate the transition probability here since the singlet/triplet crossing has no nuclear or derivative coupling (in contrast to a singlet−singlet crossing). In addition to that, the calculated electronic coupling of 20−30 cm^{-1} falls into the "nonadiabatic" regime, which is estimated to apply for energy gaps of around 0.025 eV (200 cm^{-1}) or less.[23] On the basis of the calculated SOC values and potential-energy surfaces, the value of P^{ISC} estimated at **STC$_3$** is approximately 0.001. Thus, the ISC process is non-negligible in wide regions of the singlet manifold along the reaction coordinate that controls the ultrafast internal conversion to the ground state.

Fate of the Triplet Species (Characterization and Decay to the Ground State). After the ISC, the molecule decays to the triplet surface to yield $^3(\pi,\pi^*)_{min}$. In this structure, the excitation is localized on the C_5-C_6 π bond of the molecule, and the bond is very twisted. Thus, along the decay to the T_1 hypersurface, the excitation changes character, and the resulting biradical localized on the C_5-C_6 π bond is consistent with the currently accepted dimerization reaction through the triplet state.[6] In the region of $^3(\pi,\pi^*)_{min}$, we have optimized two minima which correspond to different conformers of this species, with approximately the same energy (see Supporting Information). Moreover, in the vicinity of these structures, we have optimized two structures of T_1/S_0 crossing for decay of the triplet to the ground state ($(T_1/S_0)_X$, Figure 1b), which are different conformational minima in the (N-1)-dimensional space of T_1/S_0 degeneracy. All structures have the same electronic character but different ring conformation. The crossing has a sloped topology, and it can be accessed from $^3(\pi,\pi^*)_{min}$ after further twisting around the C_5-C_6 bond (see the direction indicated by the arrows in Figure 1b). The barrier to $(T_1/S_0)_X$ is estimated to be around 5 kcal mol^{-1} (0.2 eV), and the calculated SOC along the MEP from $^3(\pi,\pi^*)_{min}$ to $(T_1/S_0)_X$ is approximately 1 cm^{-1}. ISC to S_0 regenerates cytosine in its ground state, as confirmed by an MEP calculation on S_0 (see Supporting Information). The crossing $(T_1/S_0)_X$ can be rationalized in terms of the geometry changes that take place on the carbon−carbon double bond of cytosine, which can be related to those occurring in the T_1-S_0 ISC of ethene itself.[24] It is well-known that the SOC vanishes for planar ethene and 90°-twisted ethene and has a maximum value at 45°. For cytosine, at the CASSCF optimized geometry $(T_1/S_0)_X$, the dihedral angle is about 125°, which is close to the angle for which SOC is maximal in ethene. In fact, this latter value is of the same order of magnitude as the one calculated here for cytosine. It is fascinating to realize that the geometries close to the singlet/triplet crossings are precisely the ones that favor the intersystem crossing mechanism by increasing the SOC elements.

Conclusions

In conclusion, along the relaxation pathway of singlet-excited cytosine, ISC may take place populating the lowest triplet state. The overall picture is schematically shown in Figure 1. Upon light absorption, S_1 is populated since it carries most of the intensity in the low-energy spectral region. Along the S_1 relaxation path, a minimum is reached and fluorescence can occur, although the most favored route is toward the radiationless channel involving the S_1/S_0 crossing (Figure 1a). Close to the MEP for radiationless decay of S_1, there is a region of S_1/T_1 degeneracy with substantial SOC. In this manner, the lowest triplet state can be populated. The $T_1(\pi,\pi^*)$ state can subsequently be involved in further reactions, emit, or become deactivated to S_0 if enough vibrational energy is available (Figure 1b). In fact, the topology formed by $^3(\pi,\pi^*)_{min}$ and $(T_1/S_0)_X$ is very similar to the one found for the guanine−cytosine base pair when the triplet excitation is localized in cytosine.[9]

In a semiclassical picture, singlet-excited cytosine passes through the region of S_1/T_1 degeneracy before decay to the ground state, and there is a non-negligible probability of ISC to the triplet state. The probability of ISC (P^{ISC}) for a single passage through the ISC region, estimated at **STC$_3$**, is approximately 0.001. Moreover, possible recrossing to S_2 (see the S_2/S_1 crossing along the MEP, Figure 3)[3] may increase the probability of ISC because along the final part of the MEP, the S_2-T_1 energy gap remains small. A more detailed assessment of the branching ratio between decay to the ground state and ISC can only be given by dynamics calculations.

Overall, ISC leads to $^3(\pi,\pi^*)_{min}$, which we propose to be the experimentally detected dark intermediate. The alternative explanation of a dark $^1(n,\pi^*)$ state intermediate seems less plausible. Thus, the $^1(\pi,\pi^*)$ and $^1(n_O,\pi^*)$ states are coupled by the pyramidalization coordinate, and there is no $^1(n_O,\pi^*)$ minimum that could act as a reservoir for the detected excited-state intermediate. Moreover, in the REMPI experiment of cytosine, the delay between the analysis laser and the ionizing laser was kept long enough (20 ns) to allow for internal conversion, as well as to ionize the largest amount of triplet population.[11] Thus, we present an "intrinsic" mechanism for the formation of the triplet state in the cytosine base without the intermediacy of photosensitizers. It is conceivable that a similar mechanism operates in thymine and uracil, which also have the carbonyl group which is the key structural element in the process described here for cytosine. In fact, a recent theoretical study indicates that the radiationless S_1/S_0 decay in uracil also follows a pyramidalization coordinate.[25] A more detailed study of thymine and uracil will be necessary to assess the relevance of the present ISC mechanism for these molecules and to identify the factors responsible for their higher cyclobutadipyrimidine yields in comparison to those of cytosine. Moreover, the present mechanism could be also relevant for the dimerization reaction of pyrimidine bases in DNA. However, the photophysics of oligomers and the various DNA forms depend greatly on stacking, and the role of the monomer excited states has to be clarified to evaluate this possibility.

(22) Klessinger, M.; Michl, J. *Excited States and Photochemistry of Organic Molecules*; VCH Publishers: New York, 1995.
(23) Farazdel, A.; Dupuis, M.; Clementi, E.; Aviram, A. *J. Am. Chem. Soc.* **1990**, *112*, 4206−4214.
(24) Klessinger, M. In *Theoretical Organic Chemistry − Theoretical and Computational Chemistry*; Párkányi, C., Ed.; Elsevier Science B. V.: Amsterdam, 1998; Vol. 5, pp 581−610.
(25) Matsika, S. *J. Phys. Chem. A* **2004**, *108*, 7584−7590.

Acknowledgment. The research reported has been supported by Project BQU2001-2926 of the Spanish MCyT and the Generalitat Valenciana (GV04B-228). L.B. is financed by the Ramón y Cajal program from the MCyT and by Grants BQU2002-04112-C02-02 and BQU2002-03334 from the Dirección General de Investigación (MCyT).

Supporting Information Available: Additional computational details and Cartesian geometries of the structures. This material is available free of charge via the Internet at http://pubs.acs.org.

JA044371H